Nature, Structure and Strength of the Acidic Sites of Amorphous Silica Alumina: An IR and NMR Study

G. Crépeau,[†] V. Montouillout,[†,‡] A. Vimont,[†] L. Mariey,[†,§] T. Cseri,[||] and F. Maugé*,[†]

Laboratoire de Catalyse et Spectrochimie, UMR CNRS, ENSICAEN, University of Caen, 14050 Caen Cedex, France, Centre de Recherche sur les Matériaux à Haute Température, UPR CNRS 4212, 45071 Orléans Cedex, France, Equipe de Recherche en Physico-chimie et Biotechnologies, EA 3914, IUT-UFR de Sciences, 14032 Caen Cedex, France, and Institut Français du Pétrole, IFP - Lyon, Direction Catalyse et Séparation, Département Catalyse Hétérogène, 69390 Vernaison, France

Received: April 11, 2006; In Final Form: June 8, 2006

IR spectroscopy of probe molecules (pyridine, 2,6-dimethylpyridine, and CO) as well as high-resolution solid state NMR and especially double-resonance experiments give a new insight into the acidic sites of amorphous silica alumina (ASA). ASA samples are heterogeneous compounds that contain a silica alumina mixed phase as well as aluminum clusters and pure silica zones. The distribution of various forms depends both on the preparation method and on the Si/Al ratio. Formation of mixed phase leads to the creation of acidic hydroxyl groups of various strength, up to that present in dealuminated HY zeolite. Detailed spectroscopic analyses show that these acidic OH groups correspond to the silanol groups located in close vicinity to an Al atom in tetrahedral environment. The strength of the acidity of the OH species of ASA could be modified both by the location of the vicinal Al atom on the surface or in the bulk and by the number of aluminum atoms in the vicinity of silanol group. Cogelification of high silica-containing ASA appears as the best mean to prepare homogeneous amorphous aluminosilicate, which exhibits the strongest Brønsted acidity.

Introduction

Developments of fuel market as well as specifications for more environmental-friendly products lead refiners to invest in processes for heavy oil conversion. Among them, hydrocracking is a key process that produces selectively high quality fuels with low sulfur content.[1] The Hydrocracking catalyst is a bifunctional solid, which combines hydro−dehydrogenation and acidic function. The hydro−dehydrogenation component is usually a sulfide phase, while the acidic component is generally a zeolite or an amorphous silica alumina (ASA). To obtain a good selectivity toward gas oil and kerosene, the acidity developed by hydrocracking catalysts should be moderate and significantly lower than that of zeolites. Nevertheless, too weak acidic properties lead to a catalyst of low activity. Consequently, balanced acidity is crucial to obtain high conversion and appropriate selectivity.

The use of oxides presenting moderate acidic properties as ASA is preferred to maximize middle distillate products. Recently, important developments in the synthesis of this type of oxide such as the synthesis of ASA via the sol−gel method or coprecipitation method have been reported,[2,3] or of aluminosilicates with controlled mesoporosity or micro-mesoporosity[4−7] have been reported. However, the adjustment of these new preparations to hydrocracking application requires an accurate control of their acidic properties.[8]

Therefore, the aim of this work is to determine the nature, strength, concentration and environment of acidic sites present in different ASA samples that can be used as support of the hydrocracking catalyst.

Several papers reported the analysis of acidic properties of ASA or related materials using adsorption of probe molecule followed by IR spectroscopy.[9,10] The first papers dealing with the characterization of the surface acidic sites of ASA appeared in the 70s.[11,12] In these studies, nature of the acidic sites as well as their evolution versus Si/Al ratio was examined using pyridine or CD_3CN chemisorption. These papers show that the formation of the mixed silica−alumina phase leads to the creation of acidic OH groups able to protonate pyridine. More recently, using CO adsorbed at low temperature, a detailed analysis of the nature and the strength of the acidic sites of ASA prepared via different routes was reported.[3,13,14] These studies confirm the presence of some highly acidic OH groups on ASA. However, even with the benefit of the improved signal-to-noise ratio of the last generation of the Fourier transform infrared (FTIR) spectrometers, papers report for high-silica-containing ASA samples only the presence of one main OH band located at a wavenumber equivalent to that of SiOH groups of silica, i.e., a very weakly acidic material. Thus, although several structures were proposed in the literature to account for this feature,[13,15] the exact origin of the strong Brønsted acidity of ASA is still under discussion.

IR spectroscopy is a tool of choice to characterize the acidic properties of oxides, particularly when using different basic probe molecules, which present complementary chemical and spectroscopic properties. Hence in this work, we will study adsorption of (i) pyridine, the most widely used probe on ASA, (ii) 2,6-dimethylpyridine (DMP), which presents strong affinity for weak Brønsted acid sites, and (iii) carbon monoxide, which, when adsorbed at low temperature, is particularly suited to probe the strength of acidic OH groups.

* To whom correspondence may be addressed. E-mail: francoise.mauge@ensicaen.fr.
[†] Laboratoire de Catalyse et Spectrochimie.
[‡] Centre de Recherche sur les Matériaux à Haute Température.
[§] Equipe de Recherche en Physico-chimie et Biotechnologies.
[||] Institut Français du Pétrole.

10.1021/jp062252d CCC: $33.50
Published on Web 07/15/2006

TABLE 1: Characteristics of the Studied Samples

name	wt % SiO_2	wt % Al_2O_3	preparation method	Ssp (m^2/g)
γ-Al_2O_3	0	100		273
Si30Al70	30	70	impregnation of alumina with silica gel	339
Si40Al60	40	60	impregnation of alumina with silica gel	324
Si88Al12	88	12	cogelification	449
Si94Al6	94	6	cogelification	488

High-resolution solid-state NMR is another well-established method to probe the local environment of both aluminum and proton atoms and provide important information about the solid acidity of zeolites and ASA materials. In particular, ^{1}H magic angle spinning (MAS) NMR with the development of double-resonance NMR, which combines the high-resolution ^{1}H MAS experiment with the reintroduction of the dipolar coupling, has become a relatively popular tool to identify the different OH groups present in the materials. In this work, we used a ^{27}Al MAS experiment to probe the environment of aluminum atoms, and ^{1}H $\{^{27}$Al$\}$ TRAPDOR[16] (transfer of population in double resonance) experiment to assign the different proton lines on the basis of their vicinity with Al centers. The combined use of double resonance NMR experiments and IR spectroscopy appears as a unique mean to specify the environment of protonic species in ASA.

Experimental Section

2.1. Catalysts. The ASA samples studied in the present work are either prepared at the Institut Français du Pétrole or commercial materials. They are named SiXAlY where X and Y are respectively the weight percentage in SiO_2 and in Al_2O_3 (Table 1). Si88Al12 and Si94Al6 were prepared by cogelification using sodium metasilicate and aluminum sulfate as precursors. Sulfuric acid was added to the solution to adjust the pH. The synthesis was performed at 293 K. After cogelification, the samples were washed, dried at 393 K, and calcined in dry air at 823 K. Si30Al70 and Si40Al60, which were supplied by Condea, were prepared by impregnation of alumina with silica gel. The specific surface areas were determined by the Brunauer−Emmett−Teller (BET) method. Characteristics of the studied ASA are summarized in Table 1.

2.2. NMR. High-resolution solid-state NMR experiments were conducted at 9.4 T on a Bruker AVANCE 400 spectrometer, operating at 400.33 and 104.5 MHz for ^{1}H and ^{27}Al, respectively. ^{27}Al MAS NMR spectra of hydrated samples were acquired with a MAS frequency of 15 kHz after a single, short pulse, ensuring quantitative excitation of the central transition. For ^{1}H experiments, the samples previously dehydrated at 700 K for 4 h, were placed inside a 4-mm MAS NMR rotor, under vacuum, using a home-built device, described elsewhere.[17,18] The ^{1}H MAS spectra were recorded using a rotor-synchronized Hahn-echo pulse sequence in order to remove the background signal arising from residual probehead protons. The spinning rate was fixed to 10 kHz and the evolution period to 600 μs. The ^{1}H nutation frequency was set to 59 kHz and the recycling delay to 30 s to avoid no saturation. Similar ^{1}H excitation conditions were used for ^{1}H $\{^{27}$Al$\}$ TRAPDOR experiment,[16] combined with a continuous irradiation on the quadrupolar ^{27}Al nuclei during the first evolution period of the Hahn-echo sequence (i.e., 600 μs). The ^{27}Al nutation frequency was set to 70 kHz to satisfy adiabaticity conditions. The ^{1}H and ^{27}Al chemical shifts were referenced relative to TMS and $Al(NO_3)_3$ 1 M, respectively.

2.3. IR Spectroscopy. The ASA samples were grounded, and pressed into self-supported wafers (disk of ca. 5 mg cm^{-2}). The samples were activated in situ in the IR cell. The activation treatment consists of a ramp up to a given temperature (423, 573, or 723 K) under primary vacuum. When the activation temperature was reached, the cell was pumped under secondary vacuum down to a residual pressure of 5×10^{-6} Torr. For the three activation temperatures, the heating time was kept constant, i.e., the heating rates were different: $v = 2$ °C/min for $T_{act} = 423$ K, $v = 3$ °C/min for $T_{act} = 573$ K, and $v = 3.5$ °C/min for $T_{act} = 723$ K.

Catalyst acidity was characterized by IR spectroscopy using pyridine, DMP, and CO as probe molecules. Two different IR cells were used depending on the temperature of adsorption probe molecule. For pyridine and DMP experiments, a conventional glass cell was used, while for CO experiments, a low-temperature cell was chosen. The latter IR cell is equipped with CaF_2 windows and presents double walls with a space for cooling agent (liquid nitrogen in this work).

After activation, 1 Torr of pyridine or of DMP was introduced in the cell where the wafer was maintained at 323 K (or 373 K for DMP). An adsorption temperature higher than ambient temperature was used to ensure a good diffusion of the probe molecule through the catalyst pellet. After adsorption of the probe molecule, the sample is then evacuated at increasing temperatures, up to the temperature of sample activation.

For CO-adsorption experiments, the activated sample was first cooled to 100 K under vacuum. Then, small doses of CO were introduced and IR spectra were recorded for each dose.

The spectra presented in this paper are all normalized to a constant mass of wafer ($m = 10$ mg for a disk diameter of 16 mm). The IR spectra following adsorption of probe molecule correspond to difference spectra, i.e., spectra of the samples taken in the presence of probe molecule after subtracting the spectrum before probe molecule adsorption.

The IR spectra were recorded with a FTIR Magna spectrometer from Thermo Optek. To obtain high-quality spectra (particularly in the zone 4000−3000 cm^{-1}), the spectrometer was equipped with a XT-KBr beam splitter and with a MCT/A detector. The spectra were scanned using 256 scans with a resolution of 4 cm^{-1}.

Results and Discussion

3.1. NMR Characterization. 3.1.1. Al Environment. Figure 1 shows the ^{27}Al MAS NMR spectra of the ASA samples. The spectrum of the Si94Al6 sample, containing the lower amount of aluminum shows a main signal centered at 53.4 ppm and a weaker, broader signal at around 1 ppm, respectively, attributed to 4-fold (Al^{IV}) and 6-fold (Al^{VI}) oxygen-coordinated aluminum. This suggests that, in this sample, aluminum atoms are almost exclusively in a tetrahedral environment. The signal is Gaussian like and does not exhibit a specific quadrupolar line shape. It is characteristic of a quite symmetric environment for the aluminum. The spectra of the two samples obtained by impregnation, Si40Al60 and Si30Al70, are quite similar. They are composed of two main peaks with maximum at around 60 and 5 ppm, attributed to aluminum in tetrahedral and octahedral environment. These spectra are similar to that of γ-alumina.

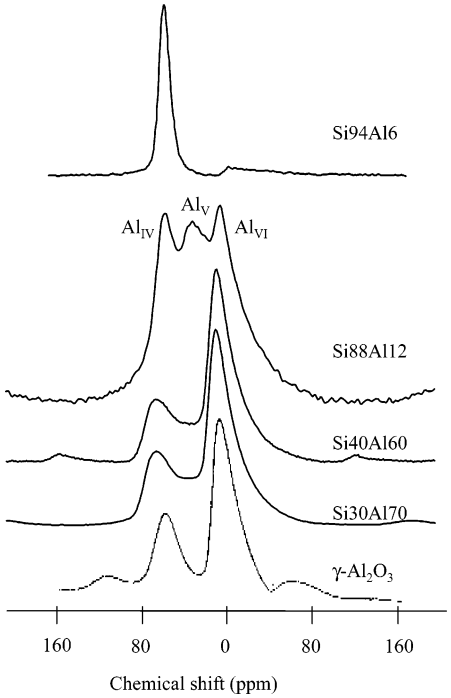

Figure 1. ^{27}Al MAS NMR spectra of ASA (B0 = 9.4 T, rotation 14 kHz).

However, the nonzero intensity between the two main lines indicates the presence of a third, weaker component, not present in alumina. The signals exhibit an asymmetric line shape with a steep low-field edge and a trailing high-field edge, characteristic of distorted environment. Finally the spectrum of the Si88Al12 sample, obtained by cogelification, exhibits clearly three components with isotropic chemical shift in the range of 60−70, 30−40, and 0−10 ppm. The signals at 60−70 and 0−10 ppm are unambiguously assigned to Al^{IV} and Al^{VI} species.[19] According to the literature,[20] the third signal (30−40 ppm) is ascribed to a pentacoordinated aluminum center. This type of environment is commonly observed in oxides obtained by sol−gel routes.[19]

All the spectra have been simulated using Dmfit software[21] to extract a precise isotropic chemical shift, mean quadrupolar coupling as well as the relative intensity of the various components. The results are summarized in Table 2. Despite the different synthesis routes used, the results indicate that the fraction of 6-fold coordinated aluminum increased with the amount of alumina. In fact, the Al^{IV}/Al^{VI} ratio is maximum at low Al concentration. Moreover, the comparison between the spectra of γ-Al_2O_3 and those of impregnated samples indicates that these samples (Si40Al60, Si30Al70) are mainly composed of a core of alumina surrounded by silica layer. By contrast, the presence of an important amount of penta and tetracoordinated aluminum in the Si88Al12 obtained by cogelification suggests a better incorporation of aluminum in the silica network.

3.1.2. Proton Environments. ^{1}H MAS spectral resolution improves with the dehydration process thus allowing the distinction between different hydroxyl groups. Moreover, it is possible to discriminate the protons adjacent to aluminum from other OH groups using double resonance experiments, such as ^{1}H {^{27}Al} TRAPDOR sequence, based on the analysis of the effect of dipolar ^{1}H/^{27}Al interaction on MAS proton spectra.

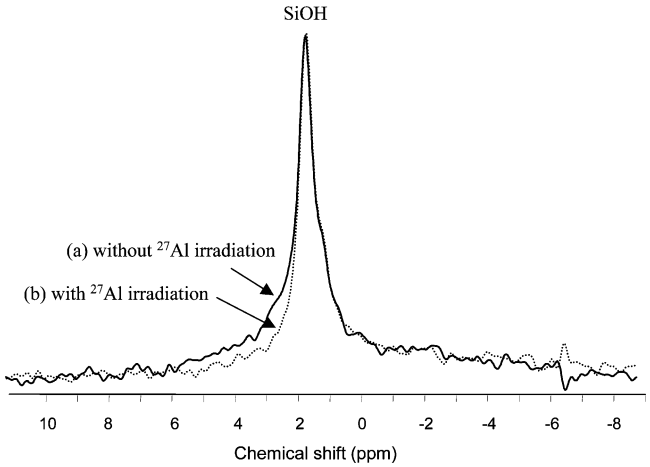

Figure 2. ^{1}H {^{27}Al} TRAPDOR experiment of Si40Al60 (B0 = 9.4 T, rotation 10 kHz). The full and the dotted lines correspond, respectively, to ^{1}H MAS spectrum acquired without and with ^{27}Al irradiation.

The ^{1}H MAS NMR spectrum of the Si40Al60 sample, previously outgassed at 700 K for 4 h, is presented in Figure 2. In addition to the main peak at 1.8 ppm, attributed to silanol groups,[22] a weak shoulder can be observed at about 2.8 ppm. No signal at 7 ppm characteristic of Brønsted acid sites Si(OH)Al was detected.[23] The assignment of the weak signal at 0.8 ppm is not straightforward. Indeed, according to the literature it can be attributed to either a SiOH group interacting with the oxygen of the framework[24] or to a AlOH species of pure γ-alumina.[25]

The environment of the two types of proton is probed using ^{1}H {^{27}Al} TRAPDOR sequence. In this experiment, the use of continuous-wave ^{27}Al irradiation during ^{1}H signal acquisition results in a loss of intensity of resonances attributed to proton in close spatial proximity with aluminum (at about 5 Å or less). The TRAPDOR experience (dotted line in Figure 2) shows that the irradiation of ^{27}Al leads to the disappearance of the shoulder centered at 2.8 ppm, while the main peak at 1.8 ppm is not affected. One may thus conclude that a small fraction of hydroxyl groups is close to aluminum atoms, while the majority of proton species are silanol groups, distant from aluminum.

3.1.3. Conclusion. The ^{27}Al NMR experiments clearly evidence the difference in aluminum local environment induced by the synthesis conditions. In the ASA prepared by impregnation of alumina by silica gel (Si30Al70, Si40Al60), the environment of aluminum atoms remains very close to that of pure alumina, in variance with the ASA prepared by cogelification (Si88Al12, Si94Al6), where indication of mixed phase was detected. At least, two types of OH groups can be distinguished on the ASA surface: silanol groups, as observed in pure silica, and hydroxyl groups close to aluminum atoms.

TABLE 2: NMR Parameters Characteristics of the Different Aluminum Environment in ASA Samples

	Al^{IV}			Al^{V}			Al^{VI}		
sample	δiso (ppm)	C_Q (MHz)	%	δiso (ppm)	C_Q (MHz)	%	δiso (ppm)	C_Q (MHz)	%
Si94Al6	55	2.3	84				7	6.7	16
Si88Al12	58	4.3	40	34	4.7	15	5	4.9	45
Si40Al30	72	5.4	30	30	2.8	4	12	4.8	66
Si60Al40	72	5.4	31	60	2.8	4	12	4.8	65

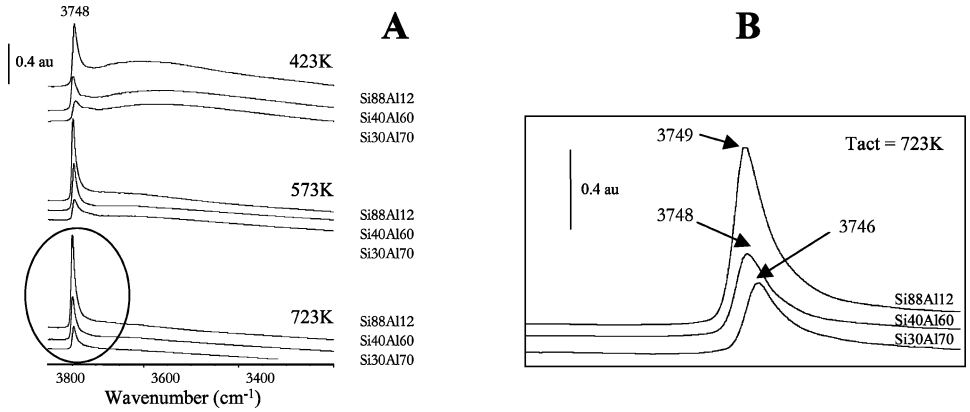

Figure 3. (A) IR spectra of the ASA activated at different temperatures. (B) Enlargement of the ν(OH) zone for the ASA activated at 723 K.

3.2. IR Characterization. The effects of the composition, preparation method and activation treatment on the acidic sites of ASA samples were examined by IR spectroscopy. The present study focuses on the ASA Si30Al70, Si40Al60, and Si88Al12 solids.

3.2.1. Hydroxyl Groups. Figure 3 presents the OH stretching zone of the different ASA after activation under vacuum at 423, 573, and 723 K. For the three samples, an asymmetric and sharp band at ~3748 cm^{-1} characteristic of silanol groups is detected.[26] The zoom on the ν(OH) band of ASA activated at 723 K shows that the SiOH band shifts from 3746 up to 3749 cm^{-1} with increasing Si content. When activation is performed at 423 K, a broad envelope, which extends from 3700 to 3300 cm^{-1}, can also be detected. This envelope completely disappears on activation at 723 K, indicating the presence of silanol groups in interaction with water molecules at low activation temperature. Indeed, the molecular water (band at 1640 cm^{-1}) is completely eliminated only for activation temperatures higher than 573 K.

It is worth noting that, even for samples containing 60 and 70 wt % of alumina, no bands characteristic of alumina ν(OH) vibrations are detected (absence of bands at 3790−80, 3775−70, 3730−25, and 3700−3675 cm^{-1}). In the literature, the absence of hydroxyl group characteristic of alumina has already been reported on ASA in the case of samples containing less than 50 wt % of alumina.[27] For ASA samples containing 75 wt % of Al_2O_3, Cairon et al. detected a shoulder at 3725 cm^{-1} and a relatively large envelope centered at 3700 cm^{-1}.[28] In our case, the absence of Al−OH band, even in the spectrum of the Si30Al70 sample, indicates a lower concentration of surface Al atoms probably due to the preparation method. Indeed, the high alumina-containing ASA of the present study were prepared by impregnation of alumina by silica gel, whereas the samples studied by Cairon et al.[28] were obtained by cogelification.

The concentration of silanol groups can be assessed using values of molar extinction coefficient of silanol band, ϵ(SiO−H) about 3 μmol^{-1} cm, previously determined by different authors.[29−31] Thus, the amount of silanol groups per square nanometer of oxide was calculated. Figure 4 reports silanol group concentrations vs silica content for the three ASA studied and compares these values to that obtained for a pure silica (SiO_2 Degussa, $S_{BET} = 450\ m^2/g$). From the comparison between the number of silanol per square nanometer and the silica content measured by chemical analysis, one can assess the surface concentration in silica. In general, the concentration of silanol groups increases with silica content, as expected from the band assignment. However, a more detailed analysis shows that, on Si88Al12, the concentration of silanol groups corresponds to that expected from chemical analysis, indicating a similar Si composition on the surface and in the core of the particles. By contrast, on Si30Al70 and Si40Al60 samples, the Si composition was higher than that expected, indicating an enrichment in silica on the surface. Such differences can be related to the synthesis methods since Si30Al70 and Si40Al60 samples are prepared by impregnation of alumina with silica gel while Si88Al12 is obtained via cogelification.

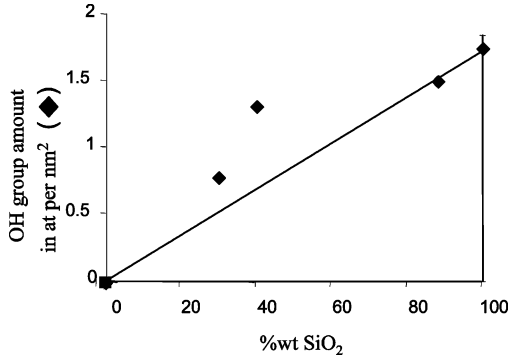

Figure 4. Evolution of the silanol group number per square nanometer with silica amount for the ASA samples and silica activated at 723 K.

3.2.2. Pyridine Adsorption. *Introduction.* Pyridine is the most commonly used probe molecule to assess the acidic sites[10] and one of the first molecules used to characterize the acidic properties of ASAs.[11,12] Pyridine presents the advantage of giving rise to very distinct vibrationnal bands according to its mode of interaction with the surface. For instance, wavenumbers of ν_{8a} and ν_{19b} bands are commonly used to discriminate pyridine coordinated to Lewis acid sites (LAS), protonated on Brønsted acid sites (BAS), or in interaction via a H bond.[32,33] Regarding the site strength, the wavenumber of the ν_{8a} band is a good indicator of the Lewis strength, whereas no information about the BAS acidic strength can be drawn from the wavenumbers of ν_{8a} and ν_{19b} bands specific of Brønsted acid sites. Such an information can, nevertheless, be obtained by study of pyridine thermodesorption.

Nature of Acidic Sites. Figure 5 presents evolution of the pyridine vibration bands vs thermodesorption temperature for Si40Al60 activated at 573 K. The other ASA samples show qualitatively very similar spectra. Three interaction modes of pyridine can be distinguished:

Protonation (PyH^+), characterized by bands at 1640, 1547, and 1492 cm^{-1}. From pyridine thermodesorption, one can note that the major fraction of the pyridinum species is eliminated on evacuation at 473−523 K. However some OH species still retain pyridine at temperature as high as 573 K, indicating the existence of a small amount of very strongly acidic OH groups.

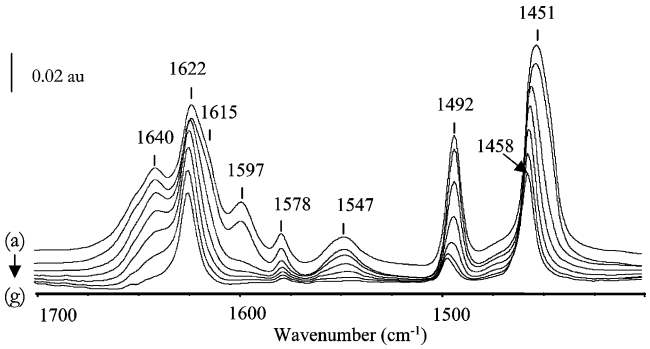

Figure 5. IR spectra of pyridine adsorbed on Si40Al60 activated at 573 K and pyridine adsorbed at 323 K and evacuated at: (a) 298 K, (b) 323 K, (c) 373 K, (d) 423 K, (e) 473 K, (f) 523 K, (g) 573 K.

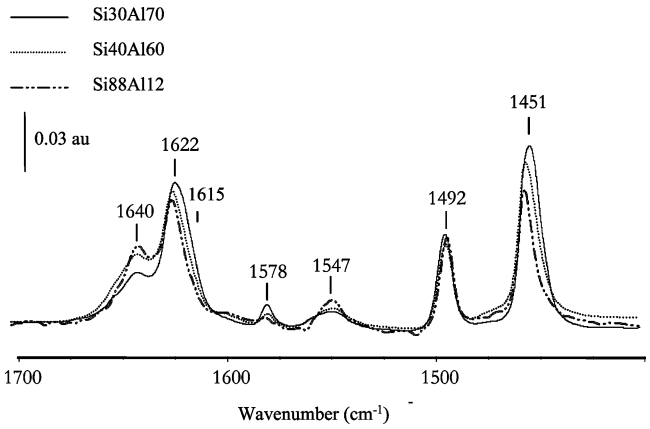

Figure 6. IR spectra of pyridine evacuated at 373 K on the ASA samples activated at 573 K.

Hydrogen bond (PyH), characterized by bands at 1597, 1492, and 1451 cm^{-1}. The band at 1597 cm^{-1} completely disappears following evacuation at 373 K, confirming its attribution to weakly interacting species.

Coordination (PyL), characterized by bands at 1622, 1615 (sh.), 1578, 1492, and 1451 cm^{-1}. After evacuation up to 423 K, the shoulder at 1615 cm^{-1} disappears, whereas the band at 1451 cm^{-1} shifts to 1458 cm^{-1}. These features indicate the presence of weak LAS. By contrast, the bands at 1622 and at 1458 cm^{-1} are still clearly observed even after evacuation at 573 K indicating the presence of very strong LAS.

It should be mentioned that, when pyridine is evacuated at temperatures higher than 473 K, no variation in the position of the bands at 1622 and 1458 cm^{-1} is observed. This is in variance with what is generally observed on pure γ-alumina where these two bands shift progressively from 1623 to 1626 cm^{-1} and from 1451 to 1456 cm^{-1} when the temperature of evacuation of pyridine increases from 373 up to 573 K.[34] The absence of shift in the position of the LAS bands when pyridine coverage decreases can be an indication of a very homogeneous environment of the strong Lewis acid sites on ASA or a weaker lateral interaction effect between adsorbed pyridine molecules due to a smaller LAS density on ASA compared to Al_2O_3.

It is also worth noting that it is not possible to specify which OH groups are responsible for the protonation of pyridine by analyzing the OH group region. Indeed, OH groups are also perturbed by pyridine coordinated species, and thus even after thermodesorption at 573 K, these species are still detected on ASA.

The effect of the chemical composition on the ASA acidic sites is presented in Figure 6. From pyridine adsorption spectra, the results show the higher the silica content, the larger the amount of BAS (1640 and 1547 cm^{-1}). Conversely, the increase of silica percentage decreases the amount of LAS (1622 and 1451 cm^{-1}). It should be mentioned that weak LAS (shoulder at 1615 cm^{-1}) are specifically diminished on the high silica sample.

Activation temperature changes the nature of ASA acidic sites. As expected, the higher the activation temperature, the larger the amount of LAS (spectra not shown). Conversely, the increase of the activation temperature decreases the amount of BAS.

3.2.3. DMP Adsorption. *Introduction.* The use of methyl-substituted pyridine such as 2,6 dimethylpyridine (DMP or lutidine) to probe the acidic properties of alumina was reported for the first time by Knözinger et al.[35,36] DMP is more basic ($pK_B = 7.3$) than pyridine ($pK_B = 8.8$), due to the presence of the two methyl groups in the α position. Consequently, DMP can protonate on more weakly acidic OH groups compared to pyridine.[37] Protonation of the DMP is clearly evidenced by the appearance of ν_{8a} and ν_{8b} bands in the 1650−1625-cm^{-1} zone (Table 3), as well as by the appearance of a δ(NH) band at 1270 cm^{-1}. With respect to the bands in the zone 1618−1603 cm^{-1}, some confusion appears in the literature about their assignment. Corma et al.[38] ascribed the band detected at 1618 cm^{-1} on γ-alumina to DMP protonated on weak Brønsted acidic sites, whereas Matulewicz et al.[39] and Morterra et al.[40] attributed it to DMP coordinated to Lewis acidic sites. The attribution of this band to DMP in interaction with weak BAS appears, however, inconsistent with several experimental observations. Indeed, the band at 1618 cm^{-1}: (i) is more clearly visible on samples activated at high temperature, (ii) is no longer observed on alumina following H_2O or H_2S adsorption,[41] and (iii) is still detected after DMP evacuation at temperature as high as 573 K. Thus, the band at 1618 cm^{-1} should be assigned to the ν_{8a} vibration of DMP coordinated to strong Lewis acid sites of alumina, i.e., on Al^{3+} in incomplete tetrahedral coordinance. On alumina, DMP adsorption also leads to the appearance of a band at 1603−1606 cm^{-1} that was assigned by Morterra et al.[40] to DMP coordinated to weaker LASs. It should be mentioned that H bonding of DMP with silanol groups also gives rise to a band at such a wavenumber (1604 cm^{-1}). Therefore, contrary to previous reports,[38] DMP can interact with various acidic sites of the surface, including with LAS. DMP is particularly well suited to distinguish the BAS from the LAS (Table 3). Difficulties arise for discriminating the nature of weak acidic sites. DMP signal is sensitive to the LAS strength. Recently, we evidenced that the $DMPH^+$ signal can also monitor the strength of the BAS.[42] Thus, the wavenumbers of ν_{8a} and ν-(NH) bands of $DMPH^+$ vary with the strength of Brønsted acidity: the lower the ν_{8a} wavenumber and the higher the ν-(NH) wavenumber, the stronger the OH acidity.

Nature of Acidic Sites. Figure 7A presents spectra of DMP adsorbed on Si40Al60 activated at 573 K in the 1700−1550-cm^{-1} region, i.e., the most characteristic zone of various DMP

TABLE 3: 2,6-DMP Vibration Frequency According to Its Mode of Adsorption (cm^{-1})

vibration modes	DMP physisorption	DMP···H	DMP-L (coordination)	DMPH+ (protonation)
ν_{8a}	1595	1600	1618−1603	1650−1640
ν_{8b}	1580	1580	1573	1630

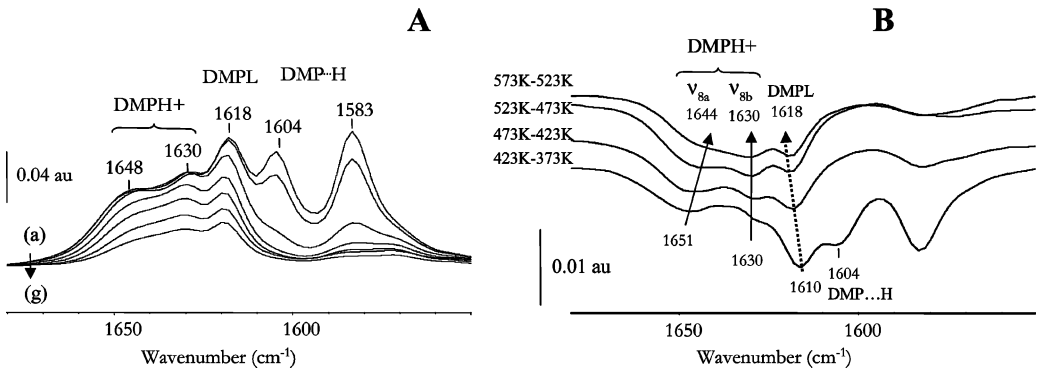

Figure 7. (A) IR spectra of DMP adsorbed on Si40Al60 activated at 573 K; DMP adsorbed at 373 K and evacuated at: (a) 298 K, (b) 323 K, (c) 373 K, (d) 423 K, (e) 473 K, (f) 523 K, (g) 573 K. (B) Difference between spectra corresponding to two successive temperatures of evacuation.

adsorption modes. On the ASA samples, three interaction modes of DMP can be distinguished:

Protonation ($DMPH^+$), characterized by the ν_{8a} and ν_{8b} bands at ~1650−1640 and 1630 cm^{-1} and by the δ(NH) band at 1270 cm^{-1}.

Coordination (DMPL), characterized by the band at ~1618 cm^{-1} and by a part of the band at 1583 cm^{-1}

Hydrogen bonding (DMPH···H) or interaction with the weak LASs, characterized by the band at 1604 cm^{-1} and by a part of the band at 1583 cm^{-1}.

Figure 7A, which presents the effect of DMP thermodesorption, shows that the bands at 1604 and 1583 cm^{-1} preferentially disappear, as expected from their assignment to DMP in weak interactions with the surface (H-bond or weak LAS). The band at 1618 cm^{-1} resists to increasing the evacuation temperature up to 573 K, in agreement with its attribution to DMP coordinated to the strong LAS. Thermodesorption leads also to a progressive decrease of the intensity of the two bands specific of protonated DMP species. However, these two bands are still observed after pumping at 573 K indicating the presence of some strong BAS on the ASA surface. In addition, one can note a shift of the ν_a $DMPH^+$ band when evacuation temperature increases.

To more accurately analyze the temperature of elimination of each DMP species, difference spectra for two successive temperatures of evacuation were also calculated (Figure 7B). Thus on this figure, the negative bands characterize the species that are eliminated in the considered temperature range. The shift of the bands characteristic of $DMPH^+$ species with evacuation temperature is more clearly visible. For mild evacuation temperatures (between 373 and 423 K), $DMPH^+$ species, which are eliminated, give rise to bands at 1651 and 1630 cm^{-1} (see negative bands). When the evacuation temperature increases, the ν_{8a} band of eliminated protonated DMP species shifts progressively down to 1644 cm^{-1}, while the wavenumber of ν_{8b} vibration remains constant (~1630 cm^{-1}). These observations are in agreement with our previous study,[42] since the lower the ν_{8a} frequency, the stronger the BAS site. The present work indicates that the ν_{8a} band of $DMPH^+$ formed on ASA contains several components and, accordingly, only DMP in interaction with the strongest acidic OH groups resists to the highest temperatures of evacuation.

Figure 8 compares the spectra of DMP adsorbed on Si40Al60 and Si88Al12 after DMP evacuation at 573 K. The two samples present bands characteristic of DMP coordinated to strong LASs (ν_{8a} band at 1618 cm^{-1}) and of $DMPH^+$ (bands in the zone 1650−1630 cm^{-1}). The absence of H-bond DMP is consistent with the high temperature of evacuation (573 K). Detailed

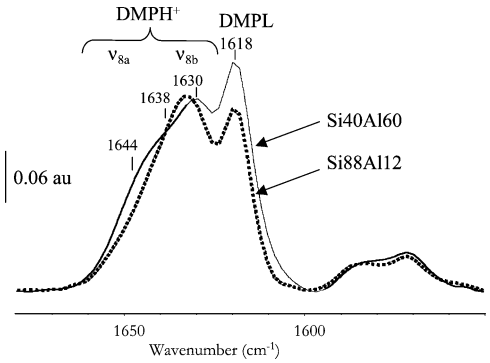

Figure 8. IR spectra of DMP evacuated at 573 K on Si40Al60 and Si88Al12 activated at 573 K.

comparison of the two DMP spectra reveals some differences in the $DMPH^+$ envelope. The high-frequency part of the $DMPH^+$ envelope on Si88Al12 does not extend up to wavenumber as high as on Si40Al60. This difference in frequency reflects the difference in acidic strength of ASA OH groups. The Si88Al12 solid exhibits stronger BASs.

In summary, DMP confirms the presence of BAS and strong LAS on the ASA, as detected by pyridine. Moreover, the wavenumber of $DMPH^+$ bands indicates that Si88Al12 exhibits a larger concentration of strong Brønsted acidic sites than low silica-containing ASA samples.

3.2.4. Carbon Monoxide Adsorption. *Introduction.* Carbon monoxide, a weak base, is a very powerful probe molecule. It can coordinate on Lewis acid sites, and if adsorbed at low temperature ($T \approx 100$ K), it can also form a H bond with acidic OH groups. Depending on its interaction mode, wavenumbers of ν(CO) bands can be directly related to the acidic strength of Lewis acid sites or hydroxyl groups. The vibration frequency of CO in interaction with LAS can reach 2230 cm^{-1} for very strong LAS and shifts down to 2157 cm^{-1} for very weak LAS. For CO in interaction with acidic OH groups, the ν(CO) frequency range is located between 2180 and 2152 cm^{-1} depending on the OH acidic strength. Thus, discriminating between CO in interaction with LAS from CO in interaction with acidic OH groups is not always staightforward from analyzing the CO stretching frequency zone. A parallel study of ν(CO) and ν(OH) zone is often necessary to distinguish between CO interaction via coordination or via H bonding. CO in interaction with OH groups of metal oxides or zeolites leads to the formation of H-bond and the extent of ν(OH) band perturbation, $\Delta\nu$(OH/CO), is proportional to the OH group acidity. As reported by Maache[43] and Cairon,[13] correlation between ν(CO) frequencies and $\Delta\nu$(OH/CO) values could be

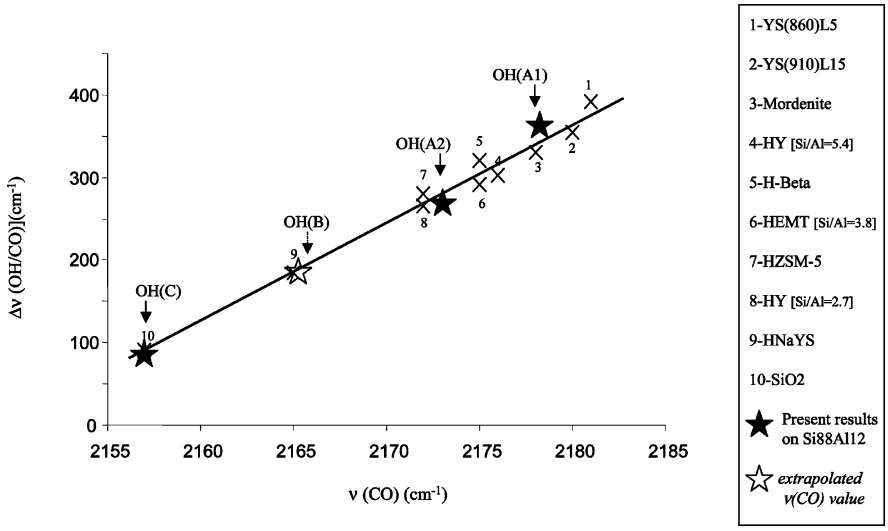

Figure 9. Relationship between $\Delta\nu$(OH/CO) shift and ν(CO) wavenumber for CO adsorbed on various zeolites and oxides: (×) values issued from literature data; (★) values obtained on ASA (solid star, when both $\Delta\nu$(OH/CO) and ν(CO) are determined in the present study; open star, when only $\Delta\nu$(OH/CO) is determined.)

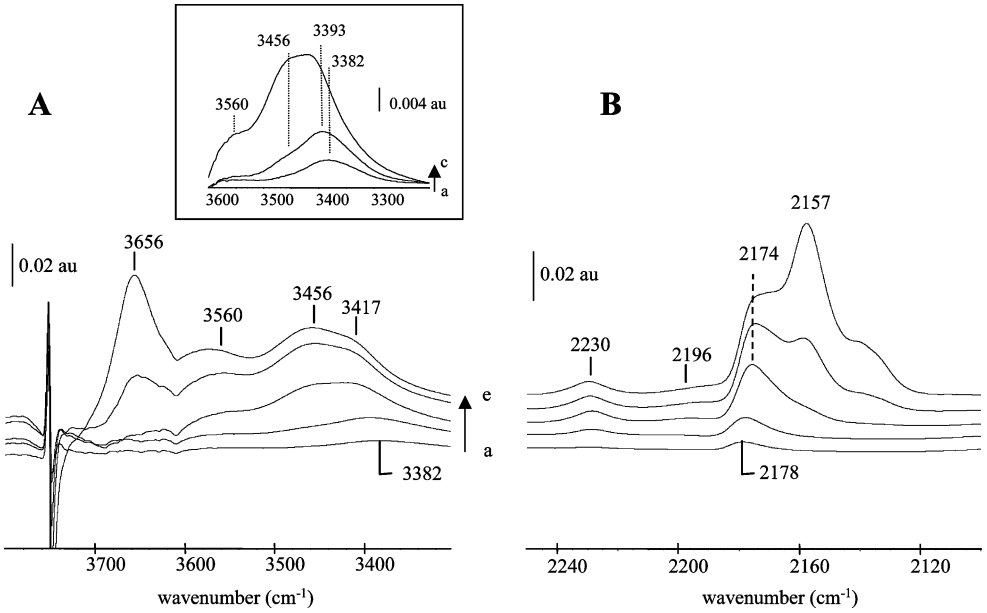

Figure 10. IR spectra of CO adsorbed on Si88Al12 activated at 723 K: (a) 10 μmol/g, (b) 30 μmol/g, (c) 80 μmol/g, (d) 160 μmol/g, (e) 260 μmol/g. (A) Zone ν(OH); (B) zone ν(CO). Inset: enlargement of the ν(OH) zone for 10, 30, and 80 μmol/g.

established for a large number of acidic materials (Figure 9). Thus, these two values are good indicators of the acidic strength of the OH groups.

Acidic Sites of Si88Al12. To determine the nature and the strength of the acidic sites of ASA and that for acidic sites eventually present in low concentrations, both very small and large doses of CO were adsorbed on the samples. In the following, we will successively analyze spectra corresponding to these two ranges of CO doses.

Figure 10 presents spectra of the adsorption of small CO doses on Si88Al12 activated at 723 K. It shows, even for the first CO dose, the partial disappearance of the 3749-cm^{-1} band. Concomitantly, a broad OH envelope appears at a lower wavenumber (Figure 10A). This envelope contains several components whose ratios vary according to the CO amount. They reveal the presence of hydroxyl groups with different acidic strengths. Indeed, the very first CO dose (10 μmol g^{-1}) adsorbed on Si88Al12 shifts a small fraction of the ν(OH) band from 3749 cm^{-1} down to 3382 cm^{-1}. After the second CO dose, the OH perturbed band appears at 3393 cm^{-1}. The introduction of additional doses leads to the appearance of a second OH perturbed component at 3456 cm^{-1}. The first OH perturbed component corresponds to a downward shift of the silanol band of 367−356 cm^{-1}, while the extent of OH perturbation of the second component is of 293 cm^{-1}. For these CO doses, only a very small fraction of isolated silanol groups is perturbed. For more important CO doses, another component appears at 3560 cm^{-1} ($\Delta\nu$(OH/CO) = 189 cm^{-1}), while an intense perturbed OH band develops at 3656 cm^{-1} ($\Delta\nu$(OH/CO) = 93 cm^{-1}), which becomes predominant for more important CO doses.

It should be noted that the difference spectrum corresponding to the introduction of the very first CO dose reveals the appearance of a positive band at 3752 cm^{-1} (Figure 10A). This upward shift indicates a small decrease of the sample temperature. Indeed, the introduction of CO in the cell improves thermal conduction between the cell reservoir full of liquid nitrogen and the wafer. This change of the sample temperature leads to a slight shift of the ASA OH bands toward higher

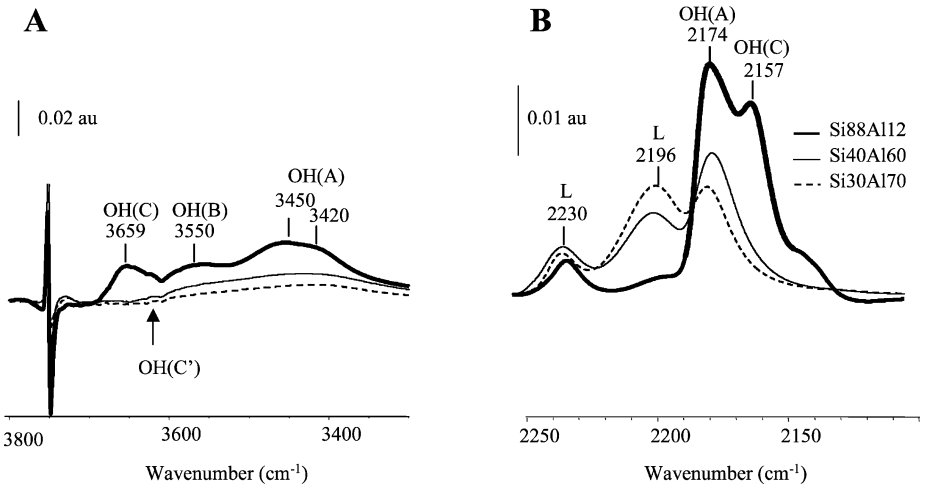

Figure 11. IR spectra of CO adsorbed (130 μmol of CO per gram of catalyst) on Si30Al70, Si40Al60, and Si88Al12 activated at 723 K. (A) Zone ν(OH); (B) zone ν(CO).

wavenumber, and thus, a part of the band at 3749 cm^{-1} shifts up to 3752 cm^{-1}.

On Si88Al12, the analysis of the ν(CO) region shows that the addition of small CO doses leads to the emergence of a band at 2178 cm^{-1} (clearly detected for the very first doses and then present as a shoulder), and of a band at 2230 cm^{-1} with a shoulder at 2196 cm^{-1}. The increase of the amount of CO introduced leads to a shift in the wavenumber of the 2178 cm^{-1} band down to 2174 cm^{-1} and to the development of a new component at 2157 cm^{-1} that increases in intensity with subsequent addition of CO doses and becomes predominant.

From their frequency range values, the ν(CO) bands at 2230 and at 2196 cm^{-1} can be attributed to CO coordination to strong and medium LAS. The attribution of the ν(CO) bands with wavenumbers lower than 2180 cm^{-1} to CO in interaction with LAS or with acidic OH groups is not always straightforward considering only their frequencies. More definite assignments can be made using the CO small doses experiments and the correlation with corresponding shift in the ν(OH) region. Thus, the ν(CO) band at 2178 cm^{-1} can be clearly assigned to CO in interaction with acidic OH groups. Indeed, first the band at 2178 cm^{-1} appears with the first CO doses, while the band at 2230 cm^{-1} is barely detectable. If the band at 2178 cm^{-1} was characteristic of coordinated CO, it should be formed after that specific of the strongest LAS (at 2230 cm^{-1}). Second, the appearance of the band at 2178 cm^{-1} correlates with the development of the OH perturbation of 367 cm^{-1}. The position of the ν(CO) band agrees with the expected OH shift from Figure 9. By use of the same methodology, the ν(CO) band at 2174 cm^{-1} can be associated to the perturbed OH band at 3456 cm^{-1} ($\Delta\nu$(OH/CO) = 293 cm^{-1}) and the band at 2157 cm^{-1} to the perturbed OH band at 3656 cm^{-1} ($\Delta\nu$(OH/CO) = 93 cm^{-1}). However, the perturbed OH band observed at 3560 cm^{-1} cannot be clearly related to a specific ν(CO) band (expected at 2165 cm^{-1} from Figure 9), because of potential overlap with adjacent CO bands at 2174 and 2157 cm^{-1} (Figure 10). Note that as shown on Figure 9 there is very good agreement between $\Delta\nu$-(OH/CO) values and corresponding ν(CO) frequency observed on acidic OH groups of ASA and those detected on oxides and zeolites.

This study shows that Si88Al12 sample exhibits:

(1) very strong acidic OH groups (sites A1) giving rise to a ν(OH)-perturbed band at 3382−93 cm^{-1}, i.e., a $\Delta\nu$(OH/CO) equal to 367−356 cm^{-1}, and a ν(CO) band at 2178 cm^{-1};

(2) strong acidic OH groups (sites A2) giving rise to a ν(OH)-perturbed band at 3456 cm^{-1}, i.e., a $\Delta\nu$ (OH/CO) equal to 293 cm^{-1}, and a ν(CO) band at 2174 cm^{-1};

(3) medium acidic OH groups (sites B) giving rise to a ν(OH)-perturbed band at 3565 cm^{-1}, i.e., a $\Delta\nu$ (OH/CO) equal to 189 cm^{-1};

(4) low acidic OH groups (sites C) giving rise to a ν(OH)-perturbed band at 3656 cm^{-1}, i.e., a $\Delta\nu$(OH/CO) equal to 93 cm^{-1} and ν(CO) band at 2157 cm^{-1};

(5) strong and medium Lewis acidic sites characterized by bands at 2230 and 2196 cm^{-1}, respectively. The presence of LAS of weak acidity could not be excluded. Indeed, the envelope at 2178−2157 cm^{-1} can contain the contribution of CO coordinated to weaker LAS in addition to the contribution of acidic hydroxyl groups.

Effect of the Composition on the Acidic Sites. Figure 11 shows the effect of catalyst composition for ASA samples activated at 723 K following adsorption of small CO doses. With respect to LAS, two types are detected on the three samples. The abundance of the LAS (2230 cm^{-1}) is constant for all Al content, whereas that of weaker strength (2196 cm^{-1}) increases with the Al amount. As for the acidity of OH group, the region of perturbed OH groups is similar on Si40Al60 and Si30Al70. Thus, the very first dose gives rise to a perturbed ν(OH) band at 3395−3400 cm^{-1}. When CO coverage increased, this band shifts to 3460−3475 cm^{-1}, while a second perturbed OH band appears at 3550 cm^{-1}. In parallel, in the CO stretching zone, a band at 2174 cm^{-1} and a shoulder at 2170 cm^{-1} are detected. These two bands are associated with the perturbed OH groups at ∼3400 and ∼3560 cm^{-1}, respectively. Thus, the three ASA samples present very strong BAS (sites A1 and A2) and medium BAS (sites B). It can be noted that the frequency of the ν(OH/CO) band corresponding to the sites A1 is located at lower value for Si88Al12 (3382 cm^{-1}) compared to that observed for Si40Al60 and Si30Al70 (3395 cm^{-1}). This reveals that the ASA which contains the highest amount of Si exhibits the strongest BAS. Note that quantitative comparison is difficult to draw from these spectra, since CO does not saturate all the acidic sites present.

Figure 12 compares the spectra obtained on the three ASA after saturation of the surface with CO (1 Torr of CO at equilibrium). This figure shows that the OH bands associated with sites of weak acidity (sites C) are predominant and increase in intensity with the silica content. This confirms that the amount of LAS with medium acidity increases with Al content.

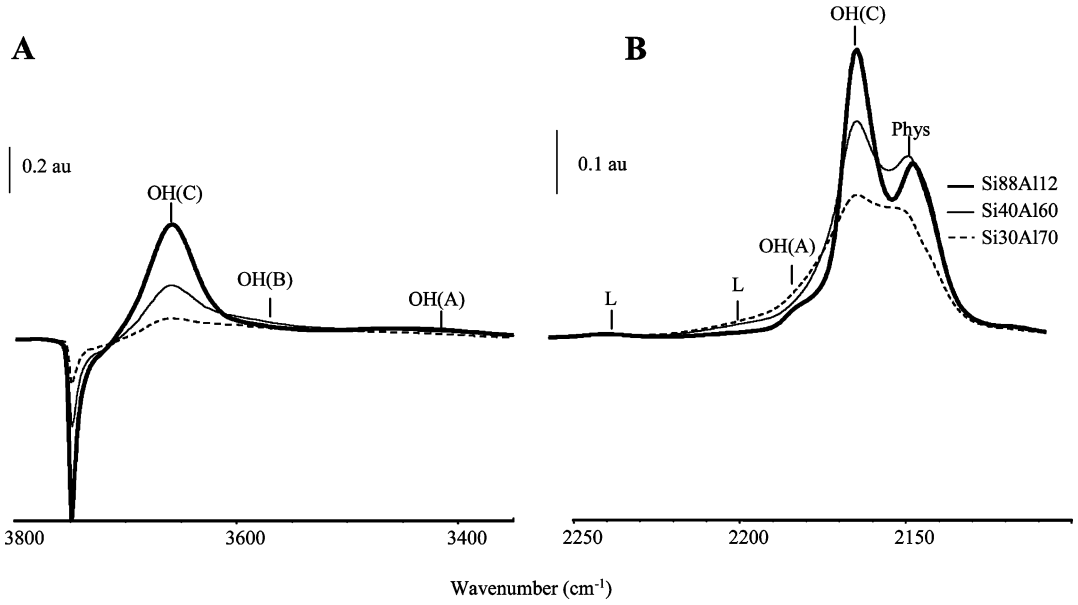

Figure 12. IR spectra of CO adsorbed (dose corresponding to the saturation of the surface in CO) on Si30Al70, Si40Al60, and Si88Al12 activated at 723 K. (A) Zone ν(OH); (B) zone ν(CO).

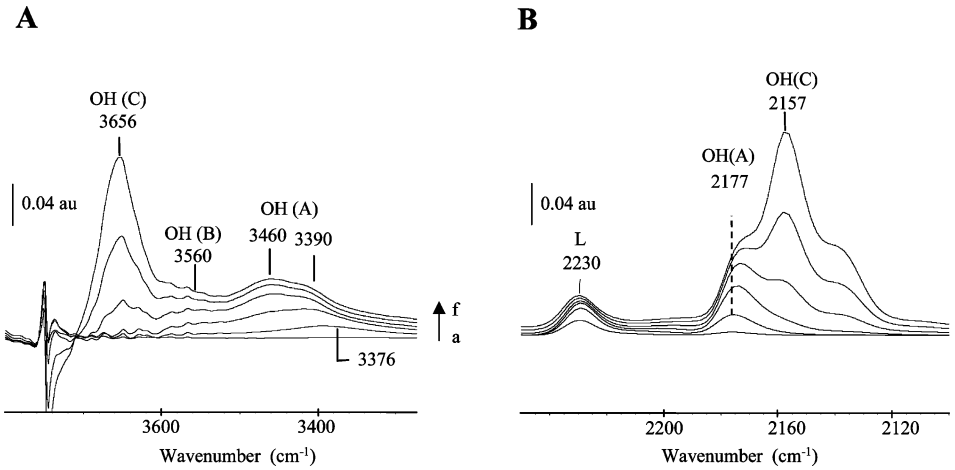

Figure 13. IR spectra of CO adsorbed on Si94Al6 activated at 723 K: (a) 30 μmol/g, (b) 90 μmol/g, (c) 170 μmol/g, (d) 290 μmol/g, (e) 440 μmol/g, (f) 590 μmol/g. (A) Zone ν(OH); (B) zone ν(CO).

Acidic Sites of Si94Al6. The Si94Al6 sample is an interesting model catalyst since this ASA contains aluminum atoms almost exclusively in a tetrahedral environment, as evidenced by ^{27}Al NMR (Figure 1). Therefore, its study should allow one to identify the environment of acidic sites.

On Si94Al6 sample (Figure 13), CO adsorption presents only one band characteristic of LAS, observed at 2230 cm^{-1}. As for the previously studied ASA samples, different types of hydroxyl groups are detected. The strongest acidic OH groups (site A1) are characterized by a perturbed OH band at 3376 cm^{-1} which shifts up to 3390 cm^{-1} ($\Delta\nu$(OH/CO) = 373−359 cm^{-1}). Sites A2 give rise to a ν(OH/CO) band at about 3460 cm^{-1} ($\Delta(\nu$(OH/CO)) = 286 cm^{-1}). Sites B correspond the perturbed OH at 3560 cm^{-1}. In addition, OH groups of weak acidity (sites C) are detected at 3656 cm^{-1}. These results illustrate the effect of catalyst composition on the OH acidic strength since the acidity of sites A1 and A2 is stronger for Si94Al6 than on Si88Al12 and greater on these high silica containing catalysts than on Si40Al60 and Si30Al70.

Effect of the Activation Temperature. The effect of the activation temperature on the acidic sites of Si30Al70 is presented in Figure 14 for small amounts of CO adsorbed. On

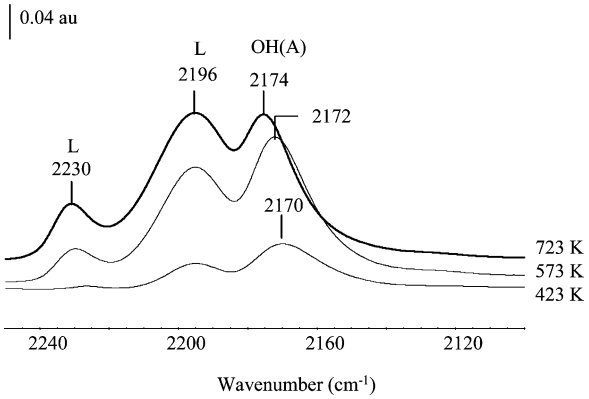

Figure 14. IR spectra of CO adsorbed (130 μmol of CO per gram of catalyst) on Si30Al70 activated at different temperatures.

Si30Al70, the interaction of CO with OH groups gives rise to a broad perturbed OH band, which does not change in aspect when the activation temperature is modified (zone not presented). However, a downward shift of the maximum of this envelope is observed when activation temperature increases from

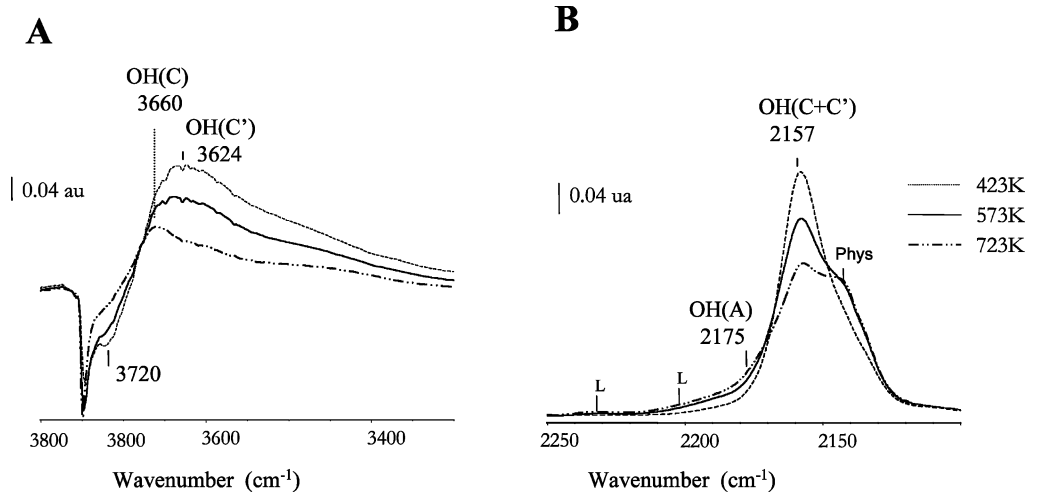

Figure 15. IR spectra of CO adsorbed (dose corresponding to the saturation of the surface in CO) on Si30Al70 activated at different temperatures. (A) Zone ν(OH); (B) zone ν(CO).

423 up to 723 K (on Si30Al70, ν(OH)/(CO) = 3420 cm^{-1} for T_{act} = 423 K and 3399 cm^{-1} for T_{act} = 723 K). In the ν(CO) region, the ν(CO) frequency of the strongest OH groups is clearly affected by the activation temperature. Thus, for the first CO dose adsorbed, the band of CO in interaction with the strongest OH groups is observed at 2170 cm^{-1} after activation at 423 K, at 2172 cm^{-1} if the sample is activated at 573 K, and appears at 2174 cm^{-1} after activation at 723 K. Hence, both ν(OH)- and ν(CO)-vibration zones illustrate the strengthening of OH groups acidity with increasing activation temperature. Regarding LAS, the amount of LAS increases with T_{act}. A close inspection of Figure 14 also shows that the strength of the strongest Lewis acidic sites is also increased (2226−2230 cm^{-1}) when activation temperature increases. Note that after activation at 423 K the 2230 cm^{-1} band is barely detectable. This can be attributed to the presence of residual water at this activation temperature, which is mainly adsorbed on the strongest Lewis acidic sites.

The same evolution with activation temperature is observed for the other silica alumina samples, i.e., increase of OH acidic strength, and of LASs number and strength with activation temperature.

When large amount of CO are adsorbed, quantitative comparison can be performed (Figures 15B and 16B). Thus, the lower the activation temperature, the larger the intensity of the ν(CO) band at 2157 cm^{-1}. This indicates an increase in the amount of weakly acidic OH groups (sites C). This increase is consistent with the larger amount of silanol groups detected in the OH zone (see section 3.2.1). Another interesting feature evidenced by Figure 16 is the increase of the amount of sites A, with increasing activation temperature.

In addition, it should be noted that the activation temperature affects the shape of the ν(OH) envelope, when perturbed by CO (Figures 15 and 16). Thus, Figures 15A and 16A show that the adsorption of CO on ASA activated at low temperature leads to the disappearance of two ν(OH) components at 3749 and 3720 cm^{-1} (negative bands). In parallel, the formation of a broad perturbed OH band at 3660(56) cm^{-1} with a shoulder at 3624 cm^{-1} (positive bands) is detected. In contrast, after evacuation at 723 K, only a band at 3749 cm^{-1} (negative band) is perturbed by CO while one H-bonded OH band appears at 3660(56) cm^{-1}. Hence in addition to site C ($\Delta\nu$(OH/CO) $\approx$ 90 cm^{-1}) previously described, a second type of weakly acidic silanol groups can be distinguished: site C′ ($\Delta\nu$(OH/CO) = 96 cm^{-1}). Thus, site C′ is slightly more acidic than site C and is more abundant for low activation temperature, i.e., when the amount of silanol group is high.

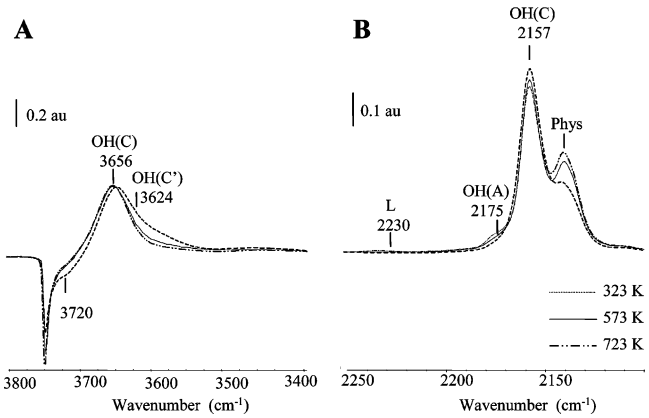

Figure 16. IR spectra of CO adsorbed (dose corresponding to the saturation of the surface in CO) on Si88Al12 activated at different temperatures. (A) Zone ν(OH); (B) zone ν(CO).

Conclusion. CO adsorption on ASA samples allows a more precise description of the surface compared to pyridine and DMP adsorption. Thus, two types of Lewis acidic sites and five types of OH groups with different acidity were evidenced.

3.3. Structure and Environment of the ASA Acidic Sites. 3.3.1. Structure of the LAS. The adsorption of pyridine, DMP, and CO on the ASA samples shows the presence of surface Al^{3+} sites with Lewis acidic properties. At least two types of LAS are evidenced: a very strong acidic LAS and a medium acidic LAS, characterized, respectively, by the bands at 1622 and 1615 cm^{-1} using pyridine adsorption and by the bands at 2230 and 2196 cm^{-1} using CO adsorption. Both probe molecules reveal that the medium LASs strongly decrease in abundance for the high silica containing sample, Si88Al12, and are no longer detected in the Si94Al6.

On pure alumina, using pyridine adsorption, Morterra et al.[44] suggested that the differences in Lewis acid strengths are due to differences in the coordination number of surface Al atoms. The presence of vacancies located on Al^{IV} sites, and $Al^{IV}-Al^{VI}$ paired sites would be responsible for the two PyL bands at 1622 and at 1615 cm^{-1}. CO adsorption on pure alumina also evidences the presence of coordination sites with different acidic strengths. In that case, it is surprising to note that papers generally related these changes to the presence of Al sites on regular planes, edges, or corners and not to sites in tetra- or

octahedral environment.[44] Regardless of the exact environment of the Al^{3+} surface sites on alumina (plane, edge, and corner sites, or Al^{IV} and $Al^{IV}-Al^{VI}$ sites), it appears that the smaller the coordination number, the stronger the Lewis acidic strength.

On the ASA studied in the present work, ^{27}Al NMR study shows the presence of Al^{IV} and Al^{VI} atoms. The Al^{IV}/Al^{VI} ratio increases with the Si amount with the Si94Al6 sample containing essentialy Al^{IV}. In addition, Si88Al12 possesses also Al^{V} sites. Thus, the absence of medium Lewis acidic sites observed on Si94Al6 appears to be associated with the quasiabsence of Al^{VI} on this sample. Similarly, the low amount of medium LAS on Si88Al12 is consistent with the low concentration of Al^{VI} sites on this sample. From these results and in agreement with the assignments proposed on pure alumina, the strongly acidic LAS can be assigned to surface Al^{IV} while the medium LAS would involve Al^{VI} sites. It should be noted that no specific acidity for the Al^{V} atoms detected on Si88Al12 is evidenced. This suggests that the Al atoms in a pentahedral environment are located in the bulk of the ASA.

In fact, Al^{IV} sites (characterized by PyL ν_{8a} at 1622 cm^{-1} and ν(CO) bands at 2230 cm^{-1}) can be present both on the mixed silica alumina phase and on the pure alumina region, whereas sites characterized by PyL ν_{8a} at 1615 cm^{-1} and ν(CO) bands at 2196 cm^{-1}, which involved Al^{VI}, are specific of the alumina domains. The distribution of these two sites depends on the Al content and on the synthesis mode. Thus, on poor aluminum containing samples (Si88Al12 and Si94Al6), which correspond to the ASA prepared by cogelification, the fraction of the silica alumina mixed phase is more important. By contrast, for high aluminum containing samples (Si30Al70 and Si40Al60), which correspond to the samples prepared by impregnation, development of alumina domains is observed. Previous ^{27}Al NMR study also shows the presence of silica alumina regions as well as alumina domains.[45]

On ASA, the amount of Lewis acidic sites increases with increasing activation temperature. Such result, which is expected on pure alumina, is surprising on ASA. Indeed on ASA, the creation of LAS cannot be explained by a surface dehydroxylation via elimination of Al−OH surface species, since such species are not detected. Therefore on ASA, the creation of Lewis acidic sites is explained by the elimination of adsorbed water on Al^{3+} sites.

3.3.2. Structure of the Weakly Acidic OH Groups of ASA. From previous studies on pure silica, at least three different environments for silanol groups were distinguished (see Scheme 1):[26]

SCHEME 1: Structures of Weakly Acidic Silanol Groups of ASA

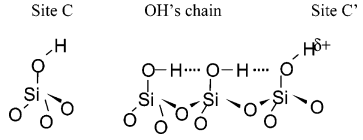

Isolated silanol groups, characterized by a ν(OH) band at 3748 cm^{-1} and ^{1}H NMR signal at 1.8 ppm. The acidity of this OH group is very weak. Indeed, CO in interaction with this specific hydroxyl group gives rise to a perturbation of the ν(OH) band, $\Delta\nu$(OH/CO) of only 90 cm^{-1}.

Silanol groups located in a chain, characterized by a ν(OH) band at $\sim$ 3715 cm^{-1}: such OH groups barely interact with a weakly basic probe molecule such as CO.

Terminal silanol groups (SiOHt), characterized by a band toward 3720 cm^{-1}: such hydroxyl groups are located at the end of a silanol chain (see Scheme 1). The interaction of the oxygen atom of the SiOHt group with a nearby OH group of the chain increases SiOHt group acidity. Indeed, CO in interaction with these terminal hydroxyl groups gives rise to a $\Delta\nu$(OH/CO) of 105 cm^{-1}. Morrow[46] showed that, on pure silica, these terminal silanol groups preferentially disappear, when the activation temperature increases up to 673 K.

Therefore, there is a great similarity between the characteristics of the weakest acidic OH groups of ASA and those of pure silica. Thus, the ν(OH) band at 3749−46 cm^{-1} to which corresponds the OH group perturbed by CO at 3656 cm^{-1} ($\Delta\nu$(OH/CO) $\approx$ 93−90 cm^{-1}), can be assigned to isolated silanol groups (called sites C). On the other hand, another ν(OH) band at 3720 cm^{-1} is specifically observed on ASA activated at low temperature. It corresponds to OH groups slightly more acidic since their perturbation by CO gives rise to a band at 3624 cm^{-1} ($\Delta\nu$(OH/CO) = 96 cm^{-1}). It can be assigned to the terminal silanol groups (called sites C′). These results suggest the presence of large silica zones in the ASA samples.

Surface composition of the ASA samples can be inferred from quantification of silanol groups and compared to what is expected from chemical analysis (Figure 4). The results show that surface composition depends on the Si/Al ratio and on the method of preparation. Oxide prepared via impregnation of alumina with silica gel presents a gradient of concentration between bulk and surface since surface Si concentration is greater on than that expected from chemical analysis. By contrast, cogelification favors mixed oxide formation.

3.3.3. Structure of the Strong Acidic OH Groups of ASA. As already reported in the literature, the most outstanding feature of ASA is the development of strong Brønsted acidic properties, which are not present on pure silica or alumina.

Indeed, a small fraction of OH groups of ASA are able to protonate pyridine and lutidine. CO adsorption allows one to determine accurately the acidic strength of these OH groups. This work reveals that the strongest OH groups (sites A1) of the studied ASA exhibit a $\Delta\nu$(OH/CO), which can reach 367 cm^{-1}, and a ν(CO) band at 2178 cm^{-1}, indicating that their acidic strength is as strong as that present in H-beta zeolite or in dealuminated Y zeolite (see Figure 9). Another fraction of these strongly acidic hydroxyl groups (sites A2) presents acidic strength ($\Delta\nu$(OH/CO) $\approx$ 293 cm^{-1}) close to that observed on non-dealuminated HY zeolite. In addition, some OH groups of medium acidity (sites B, $\Delta\nu$(OH/CO) $\approx$ 186 cm^{-1}) present an acidity close to that reported on partially alkali-exchanged faujasites.

The question of the structure and of the environment of these OH groups evidently arises. Indeed, even if the BAS of the studied ASA present acidic properties as high as those of zeolites, no evidence for the presence of hydroxyl groups bridged between silicon and aluminum atoms are observed on these solids. As a matter of fact, IR spectra (Figure 3) does not evidence any ν(OH) band at about 3630 and 3550 cm^{-1} characteristic of H−Y zeolites. ^{1}H NMR, which was shown to be more sensitive than IR spectroscopy for the detection of hydroxyl species, fails to reveal the presence of bridged OH groups.[18] Indeed, Figure 2 does not show any peaks at 3.7 and 0.1 ppm characteristic of HY zeolite. Hence on ASA samples, the IR spectrum of OH groups only presents a band characteristic of silanols at about 3746 cm^{-1} as the proton NMR spectrum that reveals that the major species are silanol groups (peak at 1.8 ppm). NMR also shows the existence of a small fraction of hydroxyl groups nearby aluminum atoms.

To explain the very strong Brønsted acidity in absence of detection of bridged OH groups, some authors proposed the presence of very broad bridged ν(OH) bands difficult to detect or even of hidden OH groups.[7,13] Indeed, broad ν(OH) bands may escape detection in a direct spectrum. However, after their perturbation or consumption by basic probe molecules interaction, they should give rise to a negative band in difference spectra (spectra of the samples taken in the presence of probe molecule after subtracting the spectrum taken before probe molecule adsorption). Such a negative band is generally more clearly observable even if it is very broad. Since no negative band is detected in the bridged OH zone, it is proposed that the acidity of silanol groups is modified by the presence of aluminum atoms in the neighboring. Thus (SiOH,Al) paired sites would generate strongly acidic Brønsted sites (Scheme 2).

SCHEME 2: Different Structures of Strongly Acidic Sites of ASA and Corresponding Acidities as Probed by CO

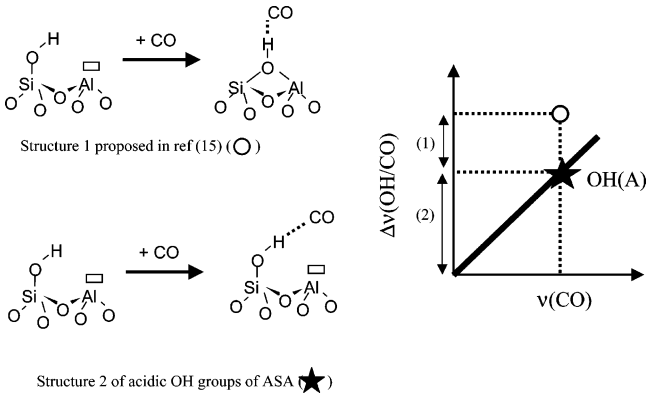

In a previous paper,[15] Trombetta et al. proposed that such entities could present strong acidity but only after a change of geometry induced by basic molecule adsorption (structure 1 of Scheme 2). Thus, SiOH groups of the structure 1 would not be acidic at the initial stage. The bridged hydroxyl groups that exhibit strong Brønsted acidity are formed by the interaction of a basic probe molecule with the silanol group in the vicinity of Al vacancy. For these authors, this structure would explain both the strong acidity measured and the lack of bridged OH groups observed in absence of basic probe molecule adsorption. In such a case, the probing of the OH group acidity by CO should give rise to a ν(CO) wavenumber equivalent to that measured on bridged SiOHAl groups of zeolites. However, as for the perturbation of the OH group by CO, the $\Delta\nu$(OH/CO) value may originate from two components (see Scheme 2): (1) the lowering of ν(SiOH) frequency due to the formation of a bridged OH group, "ν(SiOHAl)", and (2) the shift to lower wavenumber of the frequency due to the "ν(SiOHAl)" vibration on CO interaction. Thus, if the OH groups of silica alumina samples were only very acidic when bridged, the $\Delta\nu$(OH/CO) shift should be larger than the one expected from the ν(CO) value and a discrepancy between the values obtained on ASA and on zeolite would be expected. This is in variance with the results of the present study which show a good agreement between the ν(CO) values and $\Delta\nu$(OH/CO) shift obtained for ASA with the values reported in the literature on a large variety of oxides and zeolites (Figure 9). This agreement allows one to rule out the structure 1 given in ref 15 and to propose that a free silanol group located nearby an Al atom can exhibit the same acidity than that of a bridged hydroxyl group (structure 2 of Scheme 2).

In conclusion, such a result indicates that OH groups presenting similar stretching vibrations could exhibit strongly different acidities according to their environment. It is well known that the value of the OH stretching frequency is not an indicator of acidity. For example, OH groups of magnesia[47] give rise to a ν(OH) band at about 3750 cm^{-1}, i.e., a similar wavenumber than that of silica, while the OH groups of these two oxides present very different acid−base character. For a given oxide, it is generally considered that the lower the frequency, the stronger the OH group acidity; such a feature being related to an increase of the OH group coordination number. Therefore, the cases where the OH group acidic strength is changed, while both the nature of the metal cation to which the OH group is bounded stays unchanged and the coordination number of the OH group is kept constant, are particularly scarce. One example to consider is that of zeolites. Indeed, dealumination of the zeolitic framework strongly increases the OH group acidity, while the previous parameters stay constant. However, the situation is often not so simple because dealumination also causes the formation of an extraframework phase, which interacts by H bonding with the zeolitic OH groups and consequently strongly changes the zeolitic OH group frequency as well as their acidity.[13] Thus, to eliminate the effect of the amount of extraframework phase on the stretching frequency and on the acidity of the OH groups, zeolites dealuminated by isomorphous substitution or by steaming followed by leaching have been examined. It appears that, in non-dealuminated HY zeolite ($[Si/Al]_{framework} = 2.7$[48]), OH groups located in supercages give rise to a ν(OH) band at 3637 cm^{-1}, while for a zeolite dealuminated by steaming at 910 K and leached with HCl 15 M (YS(910)L15-$[Si/Al]_{framework} = 15$) as in ref 13, the band of the OH supercage is observed at 3633 cm^{-1}. As shown on Figure 9, the acidity of these OH groups strongly increases by dealumination, since the $\Delta\nu$(OH/CO) perturbation increases from 250 cm^{-1} on HY up to 350 cm^{-1} on YS(910)L15. However, the corresponding OH stretching frequency is barely modified by the dealumination of the framework. Therefore, these results provide evidence that the acidity of an OH group can be strongly modified without noticeable change of its stretching frequency.

CO adsorption also highlights the presence of at least three types of strongly acidic OH groups (sites A1, A2, and B). Different structures of (SiOH,Al^{3+}) paired sites are proposed to account for the detection of these different types of strongly acidic OH groups on ASA:

Hypothesis a: Silanol groups in the vicinity of a LAS associated with an Al atom either in a tetrahedral environment or in an octahedral environment.

Hypothesis b: Silanol groups nearby Al atom located either on the surface or in the bulk.

Hypothesis c: Silanol groups in the vicinity of Al atom(s); the amount of Al atoms in the vicinity being smaller for site A than for site B.

The Si94Al6 is a very interesting model catalyst to determine the validity of hypothesis a since almost all the aluminum atoms of this sample are in a tetrahedral environment. On the basis of this hypothesis, only one type of acidic OH groups should be detected on this sample. However, CO adsorption provides evidence for the presence of several acidic OH groups (sites A1, A2, and B) (Figure 13). Consequently, hypothesis a can be rejected. In addition, analysis of this model ASA reveals that sites A and B are all related to the presence of Al in a tetrahedral environment.

The hypothesis b concerns the location of the Al atoms of the paired sites. The sensitivity of both the concentration and the strength of sites A to the activation conditions is in favor of their attribution to a ($SiOH,Al^{IV}$) paired site that contains an Al^{3+} atom at the surface. Indeed, Figure 16 shows that increasing T_{act} increases the amount of sites A. Moreover, Figure 14 clearly indicates that the acidic strength of sites A increases when activation temperature increases (Si30Al70, Site A: $T_{act} = 423$ K, $\nu(CO) = 2170$ cm^{-1}; $T_{act} = 573$ K, $\nu(CO) = 2172$ cm^{-1}; $T_{act} = 723$ K, $\nu(CO) = 2174$ cm^{-1}). When T_{act} increases, water is eliminated, this increases the amount of unsaturated aluminum atoms in the vicinity of silanols that would lead to a modification of the charge distribution. A very simple model could explain why a ($SiOH,Al^{IV}$) paired site whose Al^{IV} is a surface site should present stronger acidity after dehydroxylation. Indeed, if the environment of tetrahedrally coordinated Al atom is complete, its positive charge, +3, should be shared by each bond, i.e., $+3/4 = +0.75$, whereas if Al atom is coordinatively unsaturated, the charge on each bond becomes $+3/3 = +1$. Thus, the stronger positive charge on the Al atom should induce a larger electron transfer via the Al−O−Si bond and therefore, should generate a greater δ^+ charge on the proton of the neighboring silanol. However, taking into account the pattern of a ($SiOH, Al^{IV}$) paired site with an Al^{IV} site located at the surface, it is not clear why basic probes do not adsorb on this LAS, thus decreasing the silanol acidity. Another possibility considered is that silanol group is located close to an Al^{IV} of the bulk (Scheme 3). In that case, a negative charge should appear on the Al atom due to its 4-fold coordinance. One possibility is that a strong acidity is generated on the proton of the closest silanol group to compensate this negative charge. But the large distance between the negative center and the proton makes the existence of such a structure questionable.

SCHEME 3: Structure of Strongly Acidic Silanol Group with nearby Al Located in the Bulk of ASA

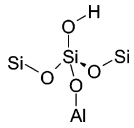

Hypothesis c is proposed by analogy with zeolites where hydroxyl group acidity increases with dealumination. CO and DMP results show that the strongest acidic OH groups are detected on the highest silica-containing samples. Indeed, stronger acid sites A are detected on Si94Al6 compared to Si88Al12. Similarly, Si88Al12 presents stronger acid sites than Si40Al60 and Si30Al70 (section 3.2.4). Therefore, silanol groups, with less Al in their environment exhibit stronger acidic OH groups.

The present study shows that the ($SiOH,Al^{IV}$) paired sites exhibit Brønsted acidity. The localization of the Al atoms either on the surface or in the bulk, as well as the amount of Al atoms in the silanol neighboring can explain the presence of SiOH groups with various Brønsted acid sites strength.

Finally, one question that needs to be addressed is why ASA presents some OH groups as acidic as those of zeolite but with a different structure. A tentative answer may lie in some structural and textural differences between ASA and zeolites. Thus, Si and Al atoms of the zeolitic framework are all located at the surface. By contrast, Si and Al in ASA can be either surface or bulk atoms. Thus the structure given in Scheme 3 cannot exist on zeolite. In addition, curved surfaces such as small pores of the zeolite should favor the formation of bridged SiOHAl groups whereas in a more open structure such as in ASA, ($SiOH,Al^{IV}$) can exist.

4. Conclusion

IR spectroscopy and high-resolution solid-state NMR allow a deep insight into the structure of ASA prepared either via cogelification or by impregnation of alumina with a silica gel.

In the ASA prepared by impregnation of alumina by silica gel, the environment of aluminum atoms remains very close to that of pure alumina. In such samples, Si concentration varies between bulk and surface and surface Si concentration is greater than that expected from chemical analysis. In contrast, the composition is more homogeneous on the ASA prepared by cogelification and the Al^{IV}/Al^{VI} ratio is greater than on impregnated ASA indicating a higher amount of mixed aluminosilicate phase.

On the two types of preparation, the ASA possess large domains of pure silica as well as zones that present strong and medium Lewis acid sites related to Al^{IV} and Al^{VI} sites as on alumina. However, the environment of LAS appears more homogeneous than on pure alumina. Al^{V} species detected by NMR analysis does not give rise to specific acidity indicating that they are not located on the ASA surface.

All the studied ASA present a low amount of very strong Brønsted acid sites, whose strength is comparable to that present on Hβ zeolite. Probing the acidic strength using CO or DMP shows that the OH acidic strength is maximum for ASA with a large Si/Al ratio and the highest Al^{IV}/Al^{VI} amount. Three salient experimental results were observed: (i) the lack of detection of other hydroxyl species except silanol groups, (ii) the excellent agreement between the $\nu(CO)$ value and the extent of silanol group perturbation by CO (Figure 9), (iii) the detection of strong BAS on ASA containing only Al in tetrahedral environment. On the basis of these results, the strong Brønsted acidity of ASA was thus related to the presence of ($SiOH,Al^{IV}$) paired sites. The differences in OH group acidic strengths was attributed to the amount of Al^{IV} in the silanol vicinity or the location of these Al^{IV} atoms.

Acknowledgment. G.C. thanks CNRS and IFP for a grant. The authors are grateful to Jean Claude Lavalley for stimulating discussions.

References and Notes

(1) Courty, Ph. *Le raffinage du pétrole, Procédés de Transformation*, Editions Technip; 1998.

(2) Parola, V. L.; Geganello, G.; Scire, S.; Venezia, A. M. *J. Solid State Chem.* **2003**, *174*, 482.

(3) Daniell, W.; Shubert, U.; Glockler, R.; Meyer, A.; Noweck, K.; Knozinger, H. *Appl. Catal A* **2000**, *196*, 247.

(4) Flego, C.; Carati, A.; Perego, C. *Microporous Mesoporous Mater.* **2001**, *733*, 44−45.

(5) Kukovecz, A.; Konya, Z.; Kiricsi, I. *J. Mol. Struct.* **2001**, *409*, 563.

(6) Bonelli, B.; Onida, B.; chen, J. D.; Galarneau, A.; Di Renzo, F.; Fajula, F.; Garrone, E. *Microporous Mesoporous Mater.* **2004**, *67*, 95.

(7) Di Renzo, F.; Chiche, B.; Fajula, F.; Viale, S.; Garonne, E. *Stud. Surf. Sci. Catal.* **1996**, *101*, 851.

(8) Ward, J. W. Hydrocracking processes and catalysts. *Fuel Process. Technol.* **1993**, *35*, 55.

(9) Zecchina, A.; Spoto, G.; Bordiga, S. *Handbook of Vibrational Spectroscopy*; Chalmers, J. M., Griffith, P. R., Eds.; Wiley: 2002; Vol. 4, p 3042.

(10) Payen, E.; Grimblot, J.; Lavalley, J.-C.; Daturi, M.; Maugé, F. *Handbook of Vibrationnal Spectroscopy*; Chalmers, J. M., Griffith, P. R., Eds.; Wiley: 2002; Vol. 4, p 3005.

(11) Ward, J. W.; Hansword, R. C. *J. Catal.* **1969**, *13*, 154.

(12) Scokart, P. O.; Declerck, F. D.; Semples, R. E.; Rouxhet, P. G. *J. Chem. Soc., Faraday Trans.* **1997**, *73*, 37.

(13) Cairon, O.; Chevreau, T.; Lavalley, J.-C. *J. Chem. Soc., Faraday Trans.* **1998**, *94*, 3039.

(14) Tsyganenko, A. A.; Manoilova, O. V.; Bulanin, K. M.; Yu Storozhev, P.; Haukka, S.; Palukka, A.; Lindblad, M. *Stud. Surf. Sci. Catal*. **2000**, *130*, 3149.
(15) Trombetta, M.; Busca, G.; Rossini, S.; Piccoli, V.; Cornaro, U.; Guercio, A.; Catani, R.; Willey, R. J. *J. Catal*. **1998**, *179*, 581.
(16) Grey, C. P.; Vega, A. *J. Am. Chem. Soc*. **1995**, *117*, 8232.
(17) Montouillout, V.; Aiello, S.; Fayon, F.; Fernandez, C. *Stud. Sci. Surf. Catal*. **2002**, *242*, 39.
(18) Gaillard, M.; Montouillout, V.; Maugé, F.; Fernandez, C. *Document Transformation Technology*; van Steen, E., Callanan, L. H., Claeys, M., Eds.; 2004; p 1679.
(19) Müller, D.; Gessner, W.; Behrens, H. J.; Scheler, G. *Chem. Phys. Lett.* **1981**, *79*, 59.
(20) Smith, M. E. *Appl. Magn. Reson.* **1993**, *4*, 1.
(21) Massiot, D.; Fayon, F.; Capron, M.; King, I.; Le Calvé, S.; Alonso, B.; Durand, J.-O.; Bujoli, B.; Gan, Z.; Hoatson, G. *Magn. Reson. Chem.* **2002**, *40*, 70.
(22) Brunner, E. *Catal. Today* **1997**, *38*, 361.
(23) Hunger, M.; Freude, D.; Pfeifer, H.; Bremer, H.; Jank, M.; Wendlandt, K. P. *Chem. Phys. Lett.* **1983**, *100*, 29.
(24) Brunner, E.; Beck, K.; Koch, M.; Heeribout, L.; Karge, H. G. *Microporous Mesoporous Mater*. **1995**, *3*, 395.
(25) Decanio, E. C.; Edwards, J. C.; Bruno, J. W. *J. Catal*. **1994**, *148*, 76.
(26) Burneau, A.; Gallas, J.-P. Vibrational spectroscopies. *The surface properties of silica*; J. Wiley: 1998.
(27) Scokart, P.-O.; Declerck, F. D.; Semples, R. E.; Rouxhet, P. G. *J. Chem. Soc., Faraday Trans*. **1997**, *73*, 372.
(28) Cairon, O. PhD Thesis, University of Caen, 1996.
(29) Galkin, G. A.; Kiselev, A. V.; Lygin, V. I. *Russ. J. Phys. Chem*. **1969**, *43*, 1117/1292.
(30) Van Cauwelaert, V. H.; Jacobs, P. A.; Uytterhoven, J. B. *J. Phys. Chem*. **1972**, *76*, 1434.
(31) Gallas, J.-P.; Lavalley, J.-C.; Burneau, A.; Barres, O. *Langmuir* **1991**, *7*, 1235.
(32) Rajagopal, S.; Marzari, J. A.; Miranda, R. *J. Catal*. **1995**, *151*, 192.
(33) Basila, M. R.; Kantner, T. R.; Rhee, K. H. *J. Phys. Chem.* **1964**, *68*, 3197.
(34) Kiviat, F. E.; Petrakis, L.*J. Phys. Chem.* **1973**, *77*, 1232.
(35) Knozinger, H.; Stolz, H. *Ber. Bunsen-Ges. Phys. Chem.* **1971**, *75*, 1055.
(36) Knozinger, H.; Krietenbrink, H.; Ratnasamy, P. *J. Catal*. **1976**, *48*, 436
(37) Lahousse, C.; Aboulayt, A.; Maugé, F.; Bachelier, J.; Lavalley, J.-C. *J. Mol. Catal*. **1993**, *84*, 283.
(38) Corma, A.; Rodellas, C.; Fornes, V. *J. Catal*. **1984**, ***88***, 374.
(39) Matulewicz, E. R. A.; Kerkhof, F. P. J. M.; Mouljin, L. A.; Reistma, H. J. *J. Colloid Int. Chem.* **1980**, *77*, 110.
(40) Morterra, C.; Cerrato, G.; Meligrana, G. *Langmuir* **2001**, *17*, 7053.
(41) Travert, A. PhD Thesis, University of Caen, 2001.
(42) Oliviero, L.; Vimont, A.; Lavalley, J.-C.; Romero Sarria, F.; Gaillard, M.: Maugé, F. *Phys. Chem. Chem. Phys.* **2005**, *7*, 1861.
(43) Maache, M. PhD Thesis, University of Caen, 1992.
(44) Morterra, C.; Magnacca, G. *Catal. Today* **1996**, *27*, 497.
(45) Omegna, A.; van Bokhoven, J. A.; Prins, R. *J. Phys. Chem. B* **2003**, *107*, 8854.
(46) Morrow, B. A.; McFarlan, A. J. *The Colloid Chemistry of Silica*; ACS Advances in Chemistry Series: 1994; Vol. 234, p 183.
(47) Coluccia, S.; Marchese, L.; Lavagnino, S.; Anpo, M. *Spectrosc. Chim. Acta* **1987**, *43A*, 12.
(48) Lavalley, J. C.; Anquetil, R.; Czyzniewska, J.; Ziolek, M. *J. Chem. Soc., Faraday Trans.* **1997**, *92*, 1263.